Synbiotics suppress colitis-induced tumorigenesis in a colon-specific cancer mouse model

Yasufumi Saito[1], Takao Hinoi[1,2,3*], Tomohiro Adachi[1], Masashi Miguchi[1], Hiroaki

Niitsu[1,4], Masatoshi Kochi[1], Haruki Sada[1], Yusuke Sotomaru[5], Naoya Sakamoto[6],

Kazuhiro Sentani[6], Naohide Oue[6], Wataru Yasui[6], Hirotaka Tashiro[1,3], Hideki Ohdan[1]

[1]Department of Gastroenterological and Transplant Surgery, Division of Medicine,
Biomedical Sciences Major, Graduate School of Biomedical & Health Sciences,
Hiroshima University, Hiroshima, Japan

[2]Department of Clinical and Molecular Genetics, Hiroshima University Hospital,
Hiroshima, Japan

[3]Department of Surgery, Division of Molecular Oncology, Institute for Clinical
Research, National Hospital Organization Kure Medical Center and Chugoku Cancer
Center, Hiroshima, Japan

[4]Vanderbilt University Medical Center, GI medicine, Nashville, Tennessee, United
States

[5]Natural Science Center for Basic Research and Development, Hiroshima University,
Hiroshima, Japan

25   [6]Department of Molecular Pathology, Hiroshima University Institute of Biomedical and

26   Health Sciences, Hiroshima, Japan

27

28

29   *Corresponding author:

30   E-mail address: thinoi@hiroshima-u.ac.jp (TH)

31

32

33

34 **Abstract**

35 Although synbiotics may be effective in maintaining remission of inflammatory bowel

36 disease, their anticarcinogenic effects are still debated. To address this issue, we

37 evaluated the effects of synbiotics, probiotics, and prebiotics on tumorigenesis using a

38 *CDX2P-Cre; Apc*$^{+/\text{flox}}$ mouse model harboring a colon-specific *Apc* knock out, which

39 develops adenoma and adenocarcinoma of the colon. Dextran sodium sulfate (DSS)-

40 administration promoted colonic tumor development in *CDX2P-Cre*; *Apc*$^{+/\text{flox}}$ mice, and

41 these tumors were associated with loss of *Apc* heterozygosity, as confirmed by

42 observation of well-differentiated adenocarcinomas with β-catenin accumulation in

43 tumor cell cytoplasm. Synbiotics-treatment suppressed dextran sodium sulfate-induced

44 colitis in *CDX2P-Cre*; *Apc*$^{+/\text{flox}}$ mice, thereby reducing mortality, and inhibited

45 tumorigenesis accelerated by DSS-administration. Conversely, neither probiotics nor

46 prebiotics had any effect on inflammation and tumorigenesis. *Lactobacillus casei* and

47 *Bifidobacterium breve* were detected in the fecal microbiota of probiotics-treated mice.

48 Synbiotics-treatment suppressed DSS-induced expression of *IL-6*, *STAT-3*, *COX-2*, and

49 *TNF-α* gene transcripts in normal colonic epithelium, indicating the possibility of

50   suppressing tumor development. Importantly, these genes may be potential therapeutic

51   targets in inflammation-associated colon cancer.

52

53   Keywords (5): synbiotics, colon cancer, colitis-associated cancer, dextran sodium

54   sulfate, mouse model

55

56

57

58

59

60

61

62

63

64

65

4

Introduction

Individuals with inflammatory bowel disease have a 10- to 40-fold increased risk of developing colorectal cancer compared with the general population. This indicates that colitis-associated cancer develops from chronically persistently inflamed mucosa, and progresses through dysplasia to adenocarcinoma. Therefore, efficacious anti-inflammatory treatment can reduce or retard the development of colorectal dysplasia and cancer in inflammatory bowel disease [1–4]. Nonetheless, the mechanisms that link these chronic inflammatory states to colorectal cancer development are largely unknown. Experimental evidence suggests that chronic inflammation creates a favorable environment for colitis-associated cancer initiation and for tumor growth promotion and progression [5,6]. Noxious compounds released during chronic colon inflammation are thought to damage DNA and/or alter cell proliferation or survival, thereby promoting oncogenesis [1,2]. New insights that suggest a direct relationship between the DNA damage response and chromosomal instability (CIN) have been provided by *in vivo* studies [7,8]. Immune cells, which often infiltrate tumors and preneoplastic lesions, produce a variety of cytokines and chemokines that propagate a

5

82   localized inflammatory response, and also enhance premalignant cell growth and

83   survival by activating signaling pathways, such as those involving IL-6/STAT3, TNF-

84   α, PGE2/COX-2, NF-κB, or MAPKs [5,8–12].

85   The pathogenesis of inflammatory bowel disease is related to inappropriate and

86   exaggerated mucosal immune responses to constituents of the intestinal flora [13,14].

87   Dextran sodium sulfate (DSS)-induced colitis is a well-established animal model of

88   mucosal inflammation that has been used in the study of ulcerative colitis pathogenesis

89   and in preclinical studies [6,11,15]. DSS is known to be directly cytotoxic to cells at

90   multiple levels, resulting in induction of colonic epithelium breakdown [6,16–20].

91   Exposure to gut flora leads to a significant increase in the expression of several

92   proinflammatory cytokines, chemokines, nitric oxide, and inducible nitric oxide

93   synthase [21–24]. Two inflammation-associated cancer mouse models induced by DSS

94   have been reported. One is the $Apc^{MIN/+}$ mouse, which shows increased intestinal

95   adenoma and adenocarcinoma increase on DSS-administration [25]. Another model

96   involves administration of azoxymethane (AOM) as a carcinogen and DSS to mice [6].

97   Previously, we demonstrated that *CDX2P 9. 5-NLS Cre; Apc$^{+/flox}$ (CPC;Apc)* mice

98   develop adenomas and carcinomas mainly in the distal colon and rectum, together with

99   a small number of cecum and small intestine adenomas [26]. In human colorectal

100   carcinoma with the CIN phenotype, there is a frequent loss of heterozygosity at loci on

101   chromosomes 5q, 17p, and 18q [27], whereas in *CPC;Apc* mice carrying constitutional,

102   heterozygous, inactivating mutations in the *Apc* gene, the wild-type *Apc* allele is

103   inactivated by loss of heterozygosity, indicating that CIN contributes to tumor

104   progression.

105   "Synbiotics" ("syn" -together and "bios" -life) are a combination of probiotic bacteria

106   and a growth-promoting prebiotic ingredient that are purported to exhibit synergism

107   [28]. Several studies have shown that synbiotics might be effective for maintaining

108   remission of inflammatory bowel disease in patients, and a previous review of

109   synbiotics indicated possible inhibitory mechanisms in colon carcinogenesis [28–34].

110   However, the anticarcinogenic effect of synbiotics is ambiguous and still under debate.

111   In Japan, the *Lactobacillus casei* strain Shirota and *Bifidobacterium breve* strain Yakult

112   have been marketed since 1935, and are common lactic acid bacteria which are

7

113   available commercially throughout the world. The probiotics and prebiotics used in this

114   study were chosen because they were found in Japan, are widely used worldwide as a

115   general supplement reported to have good effects, and are readily obtainable [35,36].

116   In this study, we created a new mouse model that promoted tumor development by

117   eliciting colitis in *CPC;Apc* mice, which experience spontaneous colon cancer. Using

118   this model, we evaluated the impact of synbiotics, probiotics, and prebiotics, and

119   examined the mechanism of tumorigenesis.

120

121

122

123

124

125

126

127

128

Materials and Methods

Ethics statement

This study was performed in strict accordance with the Guide for the Care and Use of

Laboratory Animals and the local committee for animal experiments. All animal

protocols were approved by the Committee on the Ethics of Animal Experiments of

Hiroshima University (Permit Number: 10–008). We checked the body weights of the

mice every day, and euthanized them immediately after weight loss was detected.

Surgery was performed under sodium pentobarbital anesthesia, and all efforts were

made to minimize the suffering of the mice. Mice were euthanized by CO_2 asphyxiation

as per IACUC guidelines.

Bacterial cells: probiotics and prebiotics

In this study, the *Lactobacillus casei* strain Shirota and *Bifidobacterium breve* strain

Yakult, were obtained from the Japan Collection of Microorganisms (Saitama, Japan),

and were used as probiotics [35,36]. These strains were cultured in Gifu Anaerobic

Medium broth (Nissui Pharmaceuticals, Tokyo, Japan) under anaerobic conditions

9

145   using AnaeroPack (Mitsubishi Gas Chemical, Tokyo, Japan) at 37 °C for 16 h. The

146   harvested bacterial cells were washed twice with phosphate-buffered saline (PBS) and

147   resuspended in PBS at a concentration of 1×10^8 colony-forming units/mL.

148   Suspensions were stored at -80 °C until use. 4^G-β-Galactosyl-sucrose (3.75 g/body;

149   Ensuiko Sugar Refining. Co. Ltd, Japan) was used as a prebiotic [37].

150

Animal model

152   Male *CPC;Apc* mice were used in this study in order to avoid sex bias.

153   To obtain *CPC;Apc* mice, 8-week-old *Apc^flox/flox^* females were bred with male CDX2P

154   9.5-NLS Cre males. All mice were housed under specific pathogen-free conditions.

155   Teklad Mouse Breeder Diet 8626 (Harland-Teklad) and automatically supplied water

156   were provided to all mice used in tumorigenesis experiments. The breeding room was

157   maintained at a constant temperature of 23°C±2°C, relative humidity of 50%±5%, 15-

158   20 air changes per hour, and a 12-h light/dark cycle, with lights on at 8:00 am. Four or

159   five mice were housed per cage with chopped wood bedding [38].

160　　To confirm the mouse genotype, loss of *Apc* heterozygosity was assessed by multiplex

161　　PCR using the following primers: *Apc*-P3, 5′-

162　　GTTCTGTATCATGGAAAGATAGGTGGTC-3′; *Apc*-P4, 5′-

163　　CACTCAAAACGCTTTTGAGGGTTGATTC-3′; and *Apc*-P5, 5′-

164　　GAGTACGGGGTCTCTGTCTCAGTGAA-3′. The target (580S), deletion (580D), and

165　　wild-type alleles yielded products of 314 (P3 and P4), 258 (P3 and P5), and 226 bp (P3

166　　and P4), respectively. The presence of the *CDX2* promoter region was assessed by PCR

167　　as previously described [26].

168

169　　**Induction of chronic colitis in mice; synbiotic, probiotic, and**

170　　**prebiotic treatments; and general assessment of colitis and**

171　　**tumorigenesis**

172　　Acute colitis was induced in 7- to 8-week-old mice by administering filter-purified

173　　drinking water (Millipore Corp., Billerica, MA, USA) containing 1% (w/v) DSS (MW

174　　36,000–50,000; MP Biomedicals, Solon, OH, USA) for 7 days. From day 7 onwards,

175　　the animals received normal drinking water. To induce chronic colitis, the mice were

11

176   administered 1% DSS for 7 days during weeks 8, 11, 14, and 17 [6,15]. Synbiotics,

177   probiotics, and prebiotics were orally consumed daily from 7 weeks to 20 weeks. Body

178   weight, stool consistency, and fecal blood loss were recorded daily. The number of mice

179   administrated drugs in this study was as follows; *CPC;Apc* mice (control group) was 8,

180   treated with synbiotics was 9, administrated DSS was 8, administrated DSS and treated

181   prebiotics was 7, administrated DSS and treated probiotics was 7, and administrated

182   DSS and treated synbiotics was 8. At 20 weeks of age, the entire gastrointestinal tract of

183   mice was removed immediately after euthanizing and flushed with ice-cold PBS.

184   Intestinal tissue was sliced longitudinally, and the location, number, and diameters of

185   polyps in the colon were recorded. The intestine was transferred to 10% buffered

186   formalin to be processed for histopathological studies. Consistent with the histologic

187   appearance, a hemispherical shape was assumed for large bowel polyps. We recorded

188   the location, number, and diameter of large intestinal polyps.

189

190   **Disease activity score assessment and histopathological**

191   **scoring**

12

192   Body weight loss, stool consistency, and the presence of gross blood determined by

193   fecal observation were assessed daily for each mouse to generate a weekly disease

194   activity index (DAI), as described previously [39]. Each parameter was scored as shown

195   in S1 Table. These scores were summed to obtain a DAI ranging from 0 to 12.

196   To assess DSS-induced colitis, colons were fixed in formalin and stained with

197   hematoxylin and eosin (H&E). Sections were coded for blind microscopic assessment

198   of inflammation (DSS-induced colitis). Histologic scoring was performed based on

199   three parameters, i.e., the severity of inflammation, crypt damage, and ulceration, as

200   described previously [39], with scores shown in S2 Table. The values were summed to

201   give a histological score (maximum 11). At minimum, two sections of different parts of

202   the distal colon per animal were scored.

203

204   **Immunohistochemistry**

205   We performed immunohistochemical analysis as described previously [40]. Anti-β-

206   catenin (BD Transduction Laboratories), rabbit monoclonal anti-CDX2 (clone

207   EPR2764Y; Nichirei, Tokyo, Japan), rabbit polyclonal anti-p53 (NCL-p53-CM5; Leica

13

208　Biosystems, Newcastle, UK), and rabbit monoclonal anti-Ki-67 (ab1667, Abcam plc,

209　Cambridge, UK) antibodies were used at dilutions of 1:2,000, 1:1,000, 1:200, and 1:100

210　(final concentration, 5 μ g/mL), respectively. The β-catenin, CDX2, p53, and Ki-67

211　staining positivity rates in the tumor area and normal colon epithelial cells were

212　quantified using Image J. [41, 42]

213　Total RNA extraction and quantitative real-time reverse
214　transcription-PCR analysis

215　To assess the effect of DSS and synbiotics administration on gene transcription related

216　to inflammation and carcinogenesis in background mouse mucosa, we performed

217　quantitative RT-PCR using total RNA extracted from mouse colon epithelium. Total

218　RNA was extracted from mouse normal colon epithelium using an RNeasy kit (Qiagen).

219　Quantitative real-time PCR was performed as described previously [43].

220　We used commercially available *IL-6, STAT3, NF-κB, PGE-2, COX-2,* and *TNF-α* real-

221　time RT PCR primers from Qiagen (product numbers: PPM03015A, PPM04643F,

222　PPM26197A, PPM03647E, PPM30180A, and PPM03113G-200). The primer sequences

223　used for amplification of β-*2m* (microglobulin) as an internal control were as follows:

14

224   sense 5′-TGGTCTTTCTGGTGCTTGTC-3′, anti-sense 5′ -

225   GTATGTTCGGCTTCCCATTC-3′.

226

227   Fecal bacteriological examinations

228   Feces were obtained directly from the colons of six mice in each treatment group to

229   investigate the effect of *L. casei* and *B. breve* strains on the gut microbiota. Fecal

230   samples for bacteriological analysis were acquired from pre- and post-treated mice at 20

231   weeks of age. Immediately after defecation, fecal samples were weighed and suspended

232   in nine volumes of RNAlater (Ambion Inc., Austin, TX, USA). The preparations were

233   then incubated for 10 min at room temperature. For RNA stabilization, fecal

234   homogenate (200 μL) was added to 1 mL of sterilized PBS and centrifuged at $5,000 \times g$

235   for 10 min. The supernatant was discarded and the pellet stored at -80 °C until RNA

236   extraction. RNA was isolated using a modification of the acid guanidinium thiocyanate-

237   phenol-chloroform extraction method. The resulting nucleic acid fraction was

238   suspended in 1 mL of nuclease-free water (Ambion) [44,45]. Bacterial numbers were

239   determined by reverse transcription-quantitative polymerase chain reaction (RT-qPCR).

15

240 A standard curve was generated from RT-qPCR data (using the threshold cycle [C_T]

241 method) and the corresponding cell count, which was determined microscopically with

242 4,6-diamidino-2-phenylindole (Vector Laboratories, Burlingame, CA) staining for the

243 dilution series of the standard strains [46]. To measure the bacterial populations in each

244 sample, three serial dilutions of extracted RNA were used for RT-qPCR. C_T values in

245 the linear range of the assay were applied to the standard curve to obtain the

246 corresponding bacterial cell count in each nucleic acid sample and then converted to the

247 number of bacteria per sample. The specificity of the RT-qPCR assay using group- or

248 species-specific primers was determined as described previously [44,45].

249

250 **Statistical analysis**

251 All data are expressed as means ± standard deviations (SDs). Statistical significance

252 was assessed using the Mann-Whitney U test, chi-square test, unpaired t test or Fisher's

253 exact test. Kruskal-Wallis analysis was used as a nonparametric test of multiplicity. The

254 data were considered statistically significant at $P < 0.05$. All statistical analyses were

255 performed using JMP 10 software (SAS Institute Inc., Cary, NC, USA).

256

Results

DSS-administration promotes colonic tumor development in a *CPC;Apc* mouse model and the tumors were caused by a loss of *Apc* heterozygosity

We investigated the effect of DSS-induced intestinal inflammation on large intestine

tumorigenesis using *CPC;Apc* mice. We compared a DSS-administration group with a

control group for the appearance of colon, cecum, and small intestine tumors. To assess

loss of *Apc* heterozygosity, we performed *Apc* genotyping on the tumor, normal colon

epithelium, and proximal small intestine.

Tumor number was increased in the DSS-administration group; however, there was no

significant difference between the treatment and control groups with regards to maximum

tumor diameter (tumor number [DSS vs. control]; 4 vs. 20; $P = 0.002$, tumor maximum

diameter; 6 mm vs. 5.5 mm; $P = 0.608$) (Fig 1A). In the control group, tumors generally

did not develop in the proximal large intestine; however, in DSS-administered mice,

tumors developed in the proximal region at almost the same frequency as in the distal

17

272   colon (Fig 1A). These tumors also showed a loss of *Apc* heterozygosity (Fig 1B).

273

274   **Fig 1. Evaluation of tumor formation and histological analysis.**

275   (A) Comparison of tumor number and site of occurrence in the large intestine between

276   DSS-administered *CPC;Apc* mice and control mice. Solid circles indicate a tumor of 5

277   mm or more and less than 10 mm. Blue triangles indicate a tumor less than 5 mm. Red

278   squares indicate a tumor of 10 mm or more. (B) Estimation of *Apc* loss of heterozygosity

279   by multiplex PCR. Histological analysis of tumors in DSS-administered *CPC;Apc* mice.

280   Hematoxylin and eosin-stained (C, D, E) and immunohistochemical staining of β -

281   catenin (F, G, H), CDX2 (I, J, K), p53 (L, M, N), and Ki-67 (O, P, Q). (C, F, I, L, O: 40×,

282   box with a solid line indicates a tumor; box with a broken line indicates normal colon

283   epithelium. D, G, J, M, P: tumor 200×. E, H, K, N, Q: normal colon epithelium 200×.

284

285   **Tumor induction by DSS-administration was confirmed by the**

286   **presence of well-differentiated adenocarcinomas with β-**

287   **catenin accumulation in tumor cell cytoplasm**

288   The tumors of DSS-administered mice had nuclear atypia and maintained the duct

289   structure. Almost no infiltration into the submucosal layer was observed (Fig 1C–E). a

290   high accumulation of β-catenin was observed in the tumor cell cytoplasm, whereas

291   normal colon epithelium in the mucosal crypt stained weakly for this marker (Fig 1F–H).

292   Immunostaining for CDX2 showed moderate staining in both tumor cells and normal

293   colon epithelium cells (Fig 1I–K), indicating well-differentiated tumors. Immunostaining

294   for p53 produced light staining in both tumor and normal colon epithelium (Fig 1L–N).

295   Immunostaining for Ki-67 generally showed no staining in either tumor or normal colon

296   epithelium (Fig 1O–Q). On the basis of the histological findings, the tumors elicited by

297   DSS-administration were well-differentiated adenocarcinomas with low invasive

298   behavior and low growth potential at the time of sacrifice (20 weeks of age). The analysis

299   of immunostaining positivity rates using ImageJ indicated that β-catenin, CDX2, p53,

300   and Ki-67 were present in, respectively, 9.6%, 22%, 5%, and 3% of normal colon

301   epithelial tissue. In contrast, they were present in, respectively, 88%, 30%, 10%, and 2%

302   of tumor tissue.

303

19

Synbiotics-treatment suppresses the symptoms of colitis induced by DSS, resulting in reduced mortality

To evaluate the severity of colitis, we measured changes in the body weight, survival rate, and colitis status of the mice using DAI scoring based on a combination of weight loss, rectal bleeding, and stool consistency. We evaluated the effect of one course of DSS-administration (Fig 2B), observing a weight loss of up to 2% in the DSS-administration group compared with the control. After discontinuation of DSS-administration, there was an immediate gain in weight. Therefore, we evaluated the change in body weight from day 0 to day 7, because day 7 represented the nadir of body weight. Over the course of administration, mice receiving DSS showed increased weight loss. Weight loss during the four courses of DSS-administration was 10% or more. In contrast, during the courses, synbiotics-treatment significantly suppressed weight loss by 5% or less ($P < 0.05$) (Fig 2C). In survival rate analysis, the DSS-administration group showed 50% mortality related to colitis or tumor. In contrast, a significantly lower mortality rate (10%) was observed in the DSS-administered mice receiving synbiotics-treatment (Fig 2D) ($P = 0.04$). On the other hand, probiotics and prebiotics alone resulted in a slight decrease in

20

320   weight loss and a tendency to improve survival rate compared to treatment with DSS

321   alone, but this difference was not significant. Synbiotics, administered to DSS-challenged

322   mice, reduced DAI scores by 56% compared to those for animals that received DSS alone

323   (Fig 2E) (DSS vs. DSS + synbiotics; 3.6 ± 0.35 vs. 1.6 ± 0.27, $P < 0.001$).

324

325   **Fig 2. Administration schedule of DSS, probiotics and prebiotics. Evaluation of body**

326   **weight change and survival of mice and intestinal inflammation.**

327   (A) Timetable of DSS-administration and drug-treatment with probiotics and prebiotics.

328   (B) Weight transition for DSS-administration during course 1 (day 0–21, open circle and

329   broken line: control, open circle and solid line: DSS-administered mice, solid circle and

330   solid line: DSS-administered and synbiotics-treated mice). (C) Weight change during

331   each DSS-administration course (1st to 4th) in mice administered DSS and treated with

332   probiotics and/or prebiotics (open circle: DSS-administration only, solid circle: DSS-

333   administered and synbiotics-treated mice, cross: DSS-administration and probiotics-

334   treatment, solid triangle: DSS-administration and prebiotics-treatment). (D) Percent

335   survival of each group, with treatments indicated by the same symbols shown in (C)."(E)

21

336 Disease activity index (DAI) of DSS-administered mice and mice administered DSS and

337 treated with synbiotics. *: $P < 0.01$, **: $P < 0.001$

338

Synbiotics-treatment inhibits tumor development accelerated by DSS-administration in a *CPC;Apc* mouse model

341 We investigated tumorigenesis in *CPC;Apc* mice with or without DSS-administration,

342 and in the DSS-administration + probiotics- and prebiotics-treatment groups. There was

343 no significant difference between *CPC;Apc* mice in the synbiotics treatment and those in

344 the non-treatment groups regarding tumor number ($P = 0.379$) and maximum tumor

345 diameter ($P = 0.509$) (Fig 3).

346

347 **Fig 3. Comparison of tumor number and maximum tumor diameter.**

348 (A) *CPC;Apc* mice [average tumor number, average tumor maximum diameter (n = 8);

349 4.0, 5.9], (B) *CPC;Apc* mice + synbiotics [average tumor number, average tumor

350 maximum diameter (n = 9); 3.5, 5.0], (C) *CPC;Apc* mice + DSS [average tumor number,

351 average tumor maximum diameter (n = 8); 19.5, 4.4], (D) *CPC;Apc* mice + prebiotics

22

352   (average tumor number, average tumor maximum diameter (n = 7); 21, 4.6), (E) *CPC;Apc*

353   mice + probiotics [average tumor number, average tumor maximum diameter (n = 7); 14,

354   4.6], (F) *CPC;Apc* mice + synbiotics [average tumor number, average tumor maximum

355   diameter (n = 8); 8.2, 4.5]. *: $P = 0.01$, **: $P = 0.002$

356

357   No significant differences were observed in maximum tumor diameter among the

358   experimental groups. However, there was a significant reduction (42%) in tumor number

359   in the synbiotics-treatment group compared with the group administered DSS alone (DSS

360   + synbiotics vs. DSS; 8.2 vs. 19.5: $P = 0.01$). There was no significant difference in tumor

361   number in the probiotics-alone group or the prebiotics-alone group compared with the

362   DSS-administration group (Fig 3).

363

364   **Synbiotics-treatment suppresses the inflammation of normal**

365   **colon mucosa induced by DSS-administration**

366   Histological analysis of the large intestine indicates that tumor development was

367   increased by DSS-administration and suppressed by simultaneous synbiotics-treatment

23

368   (Fig 4A–C). In addition to weight transition rate, survival rate, and DAI scoring, we

369   estimated background mucosa inflammation histologically.

370

371   **Fig 4. Analysis of background inflammation in the normal colon epithelium of DSS-**

372   **administered and synbiotics-treated *CPC;Apc* mice using hematoxylin and eosin**

373   **(H&E) staining and histological score.**

374   (A) control; *CPC;Apc* mouse. (B) *CPC;Apc* mouse administered DSS. (C) *CPC;Apc*

375   mouse administered DSS with synbiotics-treatment (yellow scale 1 cm). H&E staining of

376   normal colon epithelium (D; control, E; DSS-administered mouse, F; mouse administered

377   with DSS and treated with synbiotics: ×200, black scale 100 μm) in *CPC;Apc* mouse. (G)

378   Estimation of histological score of colon epithelium inflammation. (DSS vs. DSS +

379   synbiotics; 4.5 ± 0.7 vs. 1.9×0.6, $P < 0.01$). *: $P < 0.01$

380   Although H&E staining of normal epithelium in the control group revealed no obvious

381   inflammation of the background normal mucosa (Fig 4D), the DSS-administered group

382   showed strong inflammation and mucosal damage, including strong inflammatory cell

383   infiltration and an intermediate-to-high degree of erosion (Fig 4E). The DSS-

24

384 administration + synbiotics-treatment group showed mucosal damage and moderate

385 inflammatory cell infiltration and erosion (Fig 4F). To evaluate mouse colitis, we

386 estimated the severity of colon inflammation, including crypt damage and ulceration, in

387 the H&E-stained specimens. Synbiotics-treatment under DSS-administration decreased

388 the inflammation score compared with DSS-administration alone (Fig 4G) (DSS +

389 synbiotics vs. DSS; 1.9 ± 0.57 vs. 4.5 ± 0.69, $P < 0.01$).

390

391 *Lactobacillus casei* and *Bifidobacterium breve* are present in

392 the fecal microbiota of mice treated with synbiotics

393 The analysis of fecal microbiota shows that both *L. casei* and *B. breve* were present in

394 the treatment group, but not in the non-treatment group (Table 1). Additionally, analysis

395 of other anaerobic bacteria revealed no significant changes in the bacterial population

396 (Table 1).

397

398 **Table 1. Presence of *Lactobacillus casei* strain Shirota and *Bifidobacterium breve***

399 **strain Yakult and changes in the intestinal flora in mouse colon under**

25

administration of dextran sulfate sodium (DSS), synbiotics, *Lactobacillus* alone, and

oligosaccharide alone.

Treatment group	a	b	c	d	e	f
	control	DSS(-)/syn	DSS(+)	DSS(+)/pro	DSS(+)/pre	DSS(+)/syn
mice number (n)	3	3	6	3	4	6
Total bacteria	9.7 ± 0.6	10.0 ± 0.4	9.1 ± 0.8	9.5 ± 0.4	10 ± 0.4	9.1 ± 0.6
Obligatory anaerobe						
Clostridium coccoides group	8.9 ± 1.3	9.6 ± 0.5	8.5 ± 0.8	8.9 ± 1.0	9.8 ± 0.6	8.5 ± 0.5
C. leptum subgroup	8.3 ± 1.1	8.7 ± 0.5	8.1 ± 0.5	9.1 ± 0.9	8.6 ± 0.5	8.3 ± 0.5
Bacteroides fragilis group	7.5 ± 0.4	8.1 ± 0.4	7.3 ± 1.0	7.8 ± 0.8	7.9 ± 0.3	7.7 ± 0.8
Bifidobacterium	7.9 ± 0.8	9.0 ± 0.1	8.0 ± 1.1	8.7 ± 1.2	8.4 ± 1.3	8.3 ± 1.0
Atopobium cluster	7.7 ± 0.5	9.0 ± 0.7	8.5 ± 0.9	8.0 ± 1.0	8.1 ± 0.3	8.4 ± 0.9
Prevotella	7.2 ± 0.5	8.0 ± 0.9	7.0 ± 0.6	7.5 ± 0.9	7.8 ± 0.6	7.6 ± 0.8
C. perfringens	<2.3	<2.3	<2.3	<2.3	4.3 ± 0	<2.3
Facultative anaerobe						
Total *Lactobacillus*	8.9 ± 0.5	8.9 ± 1.0	7.0 ± 1.1	7.9 ± 1.1	7.2 ± 0.3	7.4 ± 1.3
L. gasseri subgroup	8.4 ± 0.9	8.5 ± 1.5	6.4 ± 1.2	7.8 ± 1.2	6.6 ± 0.9	6.9 ± 1.5
L. brevis	3.4 ± 0.1	3.1 ± 0.5	<2.3	2.9 ± 0	<2.3	<2.3
L. casei subgroup	<3.0	7.0 ± 1.2	<3.0	5.8 ± 0.6	<2.9	5.4 ± 1.4
L. fermentum	<4.0	<4.0	<4.0	<4.0	<4.0	<4.0
L. fructivorans	<2.3	<2.3	<2.3	<2.3	<2.3	<2.3
L. plantarum subgroup	<2.4	2.8 ± 0.1	<2.4	<2.4	<2.4	<2.4
L. reuteri subgroup	8.3 ± 0.4	7.9 ± 0.6	6.6 ± 1.3	6.8 ± 1.3	5.8 ± 0.3	6.1 ± 1.2
L. ruminis subgroup	8.1 ± 0.6	8.0 ± 0.6	6.1 ± 0.8	7.0 ± 0.9	7.0 ± 0.3	6.4 ± 1.2
L. sakei subgroup	6.6 ± 0	5.5 ± 0.4	4.6 ± 1.0	5.0 ± 1.2	3.7 ± 0.4	4.4 ± 0.3
Enterobacteriaceae	5.3 ± 0	5.5 ± 0	5.0 ± 0.8	5.2 ± 0.4	4.8 ± 0	5.8 ± 0.3
Enterococcus	7.6 ± 0.7	7.4 ± 0.5	6.3 ± 0.4	6.4 ± 0.9	6.6 ± 0.2	6.6 ± 0.6
Staphylococcus	4.4 ± 0.3	4.7 ± 0.2	4.4 ± 0.1	4.5 ± 0.7	5.2 ± 0.4	5.0 ± 1.1

Aerobes						
Pseudomonas	<2.9	<2.9	<2.9	<2.9	<2.9	<2.9
Lactobacillus casei strain Shirota	<4.9	7.0 ± 1.2	<4.9	5.8 ± 0.6	<4.9	5.8 ± 0.6
Bifidobacterium breve strain Yakult	<5.0	7.3 ± 1.2	<5.0	6.0 ± 0.1	<5.0	6.2 ± 1.0

402 Mean bacterial counts (log10 cells/g) per 1 g of feces from 3–6 mice are indicated in

403 each group.

404

405   Because the *L. casei* subgroup contains the *L. casei* strain Shirota, it was detected in the

406 administration group. The *L. brevis*, *L. ruminis*, and *L. sakei* subgroups showed a decrease

407 with DSS administration, although the differences were not significant.

408

409 **DSS-induced expression of IL-6, STAT-3, COX-2, and TNF-α**

410 **gene transcripts in normal colonic epithelium was suppressed**

411 **by synbiotics-treatment**

412   Quantitative RT-PCR using total RNA extracted from mouse colon epithelium showed

413 that, in the DSS-administration group, expression of IL-6, STAT3, COX-2, PGE-2, NF-

414   κ B was significantly increased by approximately 22- to 110-fold compared to that in

27

415   the control by DSS administration. Synbiotics treatment significantly reversed the

416   upregulation of IL-6 (63%), STAT3 (41%), COX-2 (66%), and TNF-α (Fig

417   5).

418

419   **Fig 5. Expression analysis was performed for inflammation- and tumorigenesis-**

420   **associated genes in normal colon epithelium by quantitative real-time PCR.**

421   Gene expression of total RNA samples from 20-week-old *CPC;Apc* mice (C: control,

422   n = 8), 20-week-old DSS-administered *CPC;Apc* mice (D: DSS, n = 8), and 20-week-old

423   *CPC;Apc* mice administered DSS and treated with synbiotics (DS: DSS + synbiotics, n =

424   8) was analyzed using commercial high-density oligonucleotide arrays. *: $P < 0.05$, **:

425   *P* < 0.001

426

427   # Discussion

428   Colorectal cancer in mice is chemically induced with AOM, and the most-used model

429   of colitis-associated colon cancer is induced with a combination of AOM and DSS [6].

430   To mimic known mechanisms underlying colitis and cancer in humans, genetically

28

431   engineered mouse models have been created, of which $Apc^{MIN/+}$ mice were among the

432   first, although in this model tumor development was mostly limited to the small

433   intestine [25]. Previously, we showed that intestine-specific *caudal*-related homeobox

434   transcription factor *CDX2* elements confer colon epithelium-preferential transgene

435   expression in the adult mouse, and that mice carrying a *CDX2P-NLS Cre* recombinase

436   transgene and a floxed *Apc* allele developed colorectal adenomas and carcinomas [26].

437   Morphologic and molecular studies of the mouse tumors revealed their similarity to

438   human colorectal tumors, suggesting that mice in which the *CDX2P-NLS Cre* transgene

439   is used to target *Apc* (*CPC-Apc*), and other genes of interest such as *K-ras* and *Tgfbrt2*,

440   simultaneously can be used for studies in colitis-induced colorectal cancer development.

441   In this study, we created a new inflammation-associated colon cancer mouse model by

442   treating *CPC;Apc* mice with DSS, characterized by *Apc* conditional knockout with a

443   background of CIN. Our data demonstrated the inhibitory effects of synbiotics on tumor

444   development through suppression of colitis using *CPC;Apc* mice. Tumor occurrence

445   was elicited by DSS-promoted colitis, although tumor growth was not promoted. These

446   observations are similar to the findings of a previous study using an $Apc^{MIN/+}$ mouse

29

447   model [25], in which background colitis was strongly involved in tumor development.

448   Furthermore, as the *CPC;Apc* mouse model develops adenocarcinoma in a CIN

449   background, these observations suggested that colon epithelium inflammation may

450   promote tumor development through an effect on CIN.

451   Regarding the roles of synbiotics in colon cancer prevention, the current study

452   demonstrated that synbiotics-treatment in *CPC;Apc* mice had no effect on tumorigenesis

453   in terms of either tumor number or maximum diameter without intestinal inflammation

454   induced by DSS. One possible explanation is that the mice were bred in a specific

455   pathogen-free environment that maintained a constant balance of intestinal bacteria,

456   resulting in a minimal effect of synbiotics in the mouse model of spontaneous carcinoma

457   with colon-preferential *Apc* inactivation. In contrast, the human intestinal environment is

458   exposed to various stresses, which cause aggravation of the intestinal environment and

459   colitis [34]. Based on this background, we analyzed the impact of synbiotics on

460   carcinogenesis induced by colitis. We demonstrated that treatment with synbiotics

461   suppressed enteritis more effectively than administration of either *Lactobacillus* or

462   oligosaccharides alone, thereby inhibiting inflammation-induced carcinogenesis in mice

463   that reproduced an environment close to that of human colon carcinogenesis.

464   While previous studies have reported the effects of inflammation and intestinal bacteria

465   on tumorigenesis [29,47], this inflammation-induced colon cancer mouse model based on

466   CIN is considered a more useful model to investigate the carcinogenesis of colon for two

467   reasons. First, this model does not require the use of chemicals such as carcinogens. When

468   using carcinogens such as mutation inducers, the evaluation of genes associated with

469   certain phenotypes might be difficult. The *CPC;Apc* mouse model is considered to offer

470   a more precise analysis of tumor development because it involves just a single mutation

471   (*Apc*). Second, the model enables observation of colon cancer development. Previous

472   reports showed only small intestine adenoma or adenocarcinoma in mouse models of

473   spontaneous intestinal cancer such as the $Apc^{MIN/+}$ mouse, whereas the present model is

474   considered to be superior in that it more closely reproduces the environment of human

475   colon cancer.

476   We detected *Lactobacillus* in the feces of mice in the *Lactobacillus* treatment group,

477   indicating that these bacteria reached the large intestine and persisted there. However,

478   there was no significant change in other bacterial flora following synbiotics-treatment,

31

479   suggesting that the administered *Lactobacillus* had a direct anti-inflammatory effect on

480   the colonic mucosa. Previous studies have demonstrated that using probiotics and

481   prebiotics in combination reduced the fecal pH of mice and increased the amounts of

482   short-chain fatty acids, thereby preventing mucosal damage, including that of the

483   colonic crypt cells, and further promoting regeneration [48,49]. Although we did not

484   perform the relevant evaluations in the present study, it is believed that a combined

485   administration of probiotics and prebiotics inhibits mucosal damage through the

486   abovementioned mechanism. In addition, *L. brevis* and bacteria in the *L. ruminis* and *L.*

487   *sakei* subgroups showed a decrease associated with mucosal disorder following DSS-

488   administration, and this possibly affected the acceleration of tumorigenesis. Because the

489   absence of *L. ruminis* has been reported to be correlated with lactate and butyrate

490   contents in fecal waters [50], our observations can be considered compelling evidence

491   of intestinal environmental change caused by DSS-administration. There was no

492   significant change in the bacteria of the intestinal microbial flora in both the

493   *Lactobacillus*-alone and oligosaccharide-alone groups, and thus other factors must be

494   considered to explain the effect of oligosaccharide treatment on the intestinal mucosa.

495   Through quantification of the expression levels of gene transcripts associated with

496   inflammation and tumorigenesis, we found that the expression of genes associated with

497   inflammation, such as *IL-6, STAT3, NF-κB, PGE-2, COX-2,* and *TNF-α*, increased in the

498   DSS-administration group. Among these genes, the expression of *IL-6, STAT3, COX-2,*

499   and *TNF-α* was decreased in the synbiotics-treatment group with DSS administration. IL-

500   6, STAT3, COX-2, and TNF-α have been reported to be associated with tumorigenesis

501   [9,25,51–53], which was similarly demonstrated in the present analysis using *CPC;Apc*

502   mice. Thus, tumor suppressive mechanisms that involve suppression of the transcripts of

503   these genes are considered useful subjects for future therapeutic research. For example,

504   antibody drugs for each of the gene products have already been developed; the anti-TNF-

505   α antibody drug is infliximab, and IL-6 is targeted by the anti-IL-6 antibody tocilizumab

506   as well as COX-2 inhibitors. These drugs may be expected to suppress tumor

507   development. COX-2 inhibitors and NSAIDs have been shown to reduce the risk of death

508   from colon cancer and to prevent cancer [54,55]. The use of the mouse model created in

509   this study could enable estimation of the effects of these drugs, thereby indicating

510   appropriate target and drug combinations.

511   There were some limitations to the present study. First, we were not able to evaluate

512   the impact of DSS-administration on CIN and methylation. Second, the combination of

513   probiotics and prebiotics that we used is only one of many possible combinations. Many

514   studies have investigated strains that are beneficial for intestinal inflammation and

515   immunity, and comparison of a variety of combinations is an important consideration for

516   future research [28-37]. Third, although we used normal colon mucosa to analyze the

517   expression of gene transcripts related to inflammation and tumorigenesis, stromal cells

518   were present among the mucosal epithelial cells because the tissue was collected

519   macroscopically. Therefore, we were unable to obtain a completely uniform evaluation

520   due to cell heterogeneity. Also, this study selected probiotics and prebiotics that have

521   been shown to be useful. The combination of either the *Lactobacillus casei* strain Shirota

522   or *Bifidobacterium breve* strain Yakult as probiotics and oligosaccharide as probiotics

523   may be useful for suppressing enteritis and tumor development. However, the purpose of

524   this study was not to detect the best combination of probiotics and prebiotics, and this

525   will be left for future research.

526   In conclusion, using *CPC;Apc* mice, we created an inflammation-related colon cancer

34

527 mouse model in which tumor development is promoted via colitis induced by the

528 administration of DSS. The strength of this model is that it is based on CIN with the single

529 knockout of *Apc*, and does not require the use of carcinogens. Moreover, it is

530 physiologically similar to human carcinogenesis in colorectal cancer and enables

531 observation of the effects of drug administration. Furthermore, the present study

532 demonstrates that synbiotics-treatment suppressed colitis and tumor initiation in this

533 model. The notion in the current study that synbiotics have downregulated IL-6, STAT3,

534 COX-2, and TNF-α genes, which are normally associated with inflammation and

535 tumorigenesis in colon epithelium could possibly disclose new promising therapeutic

536 avenue for patients with colitis-associated colorectal cancer.

537

538 Acknowledgements

35

Disclosures

550 The authors declare no conflicts of interest associated with this manuscript.

551

References

553 **1.** Kim YJ, Hong KS, Chung JW, Kim JH, Hahm KB. Prevention of colitis-

554 associated carcinogenesis with infliximab. Cancer Prev Res. 2010;3: 1314–1333.

555 **2.** Rosenstock E, Farmer RG, Petras R, Sivak MV Jr, Rankin GB, Sullivan BH.

556 Surveillance for colonic carcinoma in ulcerative colitis. Gastroenterology. 1985;89:

557 1342–1346.

558 **3.** Langholz E, Munkholm P, Davidsen M, Binder V. Course of ulcerative colitis:

559 Analysis of changes in disease activity over years. Gastroenterology. 1994;107: 3–11.

560 **4.** Burstein E, Fearon ER. Colitis and cancer: A tale of inflammatory cells and

561 their cytokines. J Clin Invest. 2008;118: 464–467.

562 **5.** Grivennikov SI. Inflammation and colorectal cancer: Colitis-associated

563 neoplasia. Semin Immunopathol. 2013;35: 229–244.

564 **6.** Okayasu I, Ohkusa T, Kajiura K, Kanno J, Sakamoto S. Promotion of colorectal

565 neoplasia in experimental murine ulcerative colitis. Gut. 1996;39: 87–92.

566 **7.** Bassing CH, Suh H, Ferguson DO, Chua KF, Manis J, Eckersdorff M, et al.

567 Histone H2AX. *Cell. 2003*;114: 359–370.

568 **8.** Celeste A, Difilippantonio S, Difilippantonio MJ, Fernandez-Capetillo O,

569 Pilch DR, Sedelnikova OA, et al. H2AX haploinsufficiency modifies genomic stability

570 and tumor susceptibility. Cell. 2003;114: 371–383.

571 **9.** Pikarsky E, Porat RM, Stein I, Abramovitch R, Amit S, Kasem S, et al. NF-κB

572 functions as a tumour promoter in inflammation-associated cancer. Nature. 2004;431:

573 461–466.

574 **10.** Del Reino P, Alsina-Beauchamp D, Escos A, Cerezo-Guisado MI, Risco A,

575 Aparicio N, et al. Pro-oncogenic role of alternative p38 mitogen-activated protein kinases

576   p38gamma and p38delta, linking inflammation and cancer in colitis-associated colon

577   cancer. Cancer Res. 2014;74: 6150–6160.

578   **11.**   Ghaleb AM, Laroui H, Merlin D, Yang VW. Genetic deletion of Klf4 in the

579   mouse intestinal epithelium ameliorates dextran sodium sulfate-induced colitis by

580   modulating the NF-κB pathway inflammatory response. Inflamm Bowel Dis. 2014;20:

581   811–820.

582   **12.**   Wullaert A, Bonnet MC, Pasparakis M. NF-κB in the regulation of epithelial

583   homeostasis and inflammation. Cell Res. 2011;21: 146–158.

584   **13.**   Sartor RB. The influence of normal microbial flora on the development of

585   chronic mucosal inflammation. Res Immunol. 1997;148: 567–576.

586   **14.**   Hasegawa A, Iwamura C, Kitajima M, Hashimoto K, Otsuyama K, Ogino K, et

587   al. Crucial role for CD69 in the pathogenesis of dextran sulphate sodium-induced colitis.

588   PLoS One. 2013;8: e65494.

589   **15.**   Wirtz S, Neufert C, Weigmann B, Neurath MF. Chemically induced mouse

590   models of intestinal inflammation. Nat Protoc. 2007;2: 541–546.

591   **16.**   Damiani CR, Benetton CA, Stoffel C, Bardini KC, Cardoso VH, Giunta GD, et

38

592   al. Oxidative stress and metabolism in animal model of colitis induced by dextran sulfate

593   sodium. J Gastroenterol Hepatol. 2007;22: 1846–1851.

594   **17.**   Westbrook AM, Schiestl RH. Atm-deficient mice exhibit increased sensitivity

595   to dextran sulfate sodium-induced colitis characterized by elevated DNA damage and

596   persistent immune activation. Cancer Res 2010; 70(5): 1875–1884.

597   **18.**   Laroui H, Ingersoll SA, Liu HC, Baker MY, Ayyadurai S, Charania MA, et al.

598   Dextran sodium sulfate (DSS) induces colitis in mice by forming nano-lipocomplexes

599   with medium-chain-length fatty acids in the colon. PLoS One. 2012;7: e32084.

600   **19.**   Ni J, Chen SF, Hollander D. Effects of dextran sulphate sodium on intestinal

601   epithelial cells and intestinal lymphocytes. Gut. 1996;39: 234–241.

602   **20.**   Tardieu D, Jaeg JP, Cadet J, Embvani E, Corpet DE, Petit C. Dextran sulfate

603   enhances the level of an oxidative DNA damage biomarker, 8-oxo-7,8-dihydro-2'-

604   deoxyguanosine, in rat colonic mucosa. Cancer Letts. 1998;134: 1–5.

605   **21.**   Medzhitov R. Recognition of microorganisms and activation of the immune

606   response. Nature. 2007;449: 819–826.

607   **22.**   Alex P, Zachos NC, Nguyen T, Gonzales L, Chen T, Conklin LS, et al. Distinct

608   cytokine patterns identified from multiplex profiles of murine DSS and TNBS-induced

609   colitis. Inflamm Bowel Dis. 2009;15: 341–352.

610   **23.**   Beck PL, Li Y, Wong J, Keenan CM, Sharkey KA, McCafferty D. Inducible

611   nitric oxide synthase from bone marrow-derived cells plays a critical role in regulating

612   colonic inflammation. Gastroenterology. 2007;132: 1778–1790.

613   **24.**   Naito Y, Takagi T, Handa O, Ishikawa T, Nakagawa S, Yamaguchi T, et al.

614   Enhanced intestinal inflammation induced by dextran sulfate sodium in tumor necrosis

615   factor-alpha deficient mice. J Gastroenterol Hepatol. 2003;18: 560–569.

616   **25.**   Tanaka T, Kohno H, Suzuki R, Hata K, Sugie S, Niho N, et al. Dextran sodium

617   sulfate strongly promotes colorectal carcinogenesis in Apc$^{Min/+}$ mice: Inflammatory

618   stimuli by dextran sodium sulfate results in development of multiple colonic neoplasms.

619   Int J Cancer. 2006;118: 25–34.

620   **26.**   Hinoi T, Akyol A, Theisen BK, Ferguson DO, Greenson JK, Williams BO, et

621   al. Mouse model of colonic adenoma-carcinoma progression based on somatic Apc

622   inactivation. Cancer Res. 2007;67: 9721–9730.

623   **27.**   Fearon ER, Vogelstein B. A genetic model for colorectal tumorigenesis. Cell.

624   1990;61: 759–767.

625   **28.**   Kolida S, Gibson GR. Synbiotics in health and disease. Annu Rev Food Sci

626   Technol. 2011;2: 373–393.

627   **29.**   Raman M, Ambalam P, Kondepudi KK, Pithva S, Kothari C, Patel AT, et al.

628   Potential of probiotics, prebiotics and synbiotics for management of colorectal cancer.

629   Gut Microbes. 2013;4: 181–192.

630   **30.**   Fujimori S, Gudis K, Mitsui K, Mitsui K, Seo T, Yonezawa M, et al. A

631   randomized controlled trial on the efficacy of synbiotic versus probiotic or prebiotic

632   treatment to improve the quality of life in patients with ulcerative colitis. Nutrition.

633   2009;25: 520–525.

634   **31.**   Peitsidou K, Karantanos T, Theodoropoulos GE. Probiotics, prebiotics,

635   synbiotics: Is there enough evidence to support their use in colorectal cancer surgery? Dig

636   Surg. 2012;29: 426–438.

637   **32.**   Komatsu S, Sakamoto E, Norimizu S, Shingu Y, Asahara T, Nomoto K, et al.

638   Efficacy of perioperative synbiotics treatment for the prevention of surgical site infection

639   after laparoscopic colorectal surgery: A randomized controlled trial. Surg Today. 2016;46:

479–490.

33.   Okazaki M, Matsukuma S, Suto R, Miyazaki K, Hidaka M, Matsuo M, et al.

Perioperative synbiotic therapy in elderly patients undergoing gastroenterological

surgery: A prospective, randomized control trial. Nutrition. 2013;29: 1224–1230.

34.   Gibson GR, Roberfroid MB. Dietary modulation of the human colonic

microbiota: Introducing the concept of prebiotics. J Nutr. 1995;125: 1401–1412.

35.   Asahara T, Shimizu K, Nomoto K, Hamabata T, Ozawa A, Takeda Y. Probiotic

Bifidobacteria protect mice from lethal infection with Shiga toxin-producing *Escherichia*

coli O157:H7. Infect Immun. 2004;72: 2240–2247.

36.   Asahara T, Shimizu K, Takada T, Kado S, Yuki N, Morotami M, et al. Protective

effect of *Lactobacillus casei* strain Shirota against lethal infection with multi-drug

resistant *Salmonella enterica* serovar Typhimurium DT104 in mice. J Appl Microbiol.

2011;110: 163–173.

37.   Ogata Y, Fujita K, Ishigami H, Hara K, Terada A, Hara, H, et al. Effect of a

small amount of 4^G-β-D-galactosylsucrose (lactosucrose) on fecal flora and fecal

properties. J Jpn Soc Nutr Food Sci. 1993;46: 317–323.

656 **38**.   Sasada T, Hinoi T, Saito Y, Adachi T, Takakura Y, Kawaguchi Y, et al.

657 Chlorinated water modulates the development of colorectal tumors with chromosomal

658 instability and gut microbiota in Apc-deficient mice. PLoS One. 2015;10: e0132435.

659 **39.**   Theiss AL, Vijay-Kumar M, Obertone TS, Obertone TS, Jones DP, Hansen JN,

660 et al. Prohibitin is a novel regulator of antioxidant response that attenuates colonic

661 inflammation in mice. Gastroenterology. 2009;137: 199–208.

662 **40.**   Hinoi T, Lucas PC, Kuick R, Hanash S, Cho KR, Fearon ER. CDX2 regulates

663 liver intestine–cadherin expression in normal and malignant colon epithelium and

664 intestinal metaplasia. Gastroenterology. 2002;123: 1565–1577.

665 41.   Rasband, W.S., ImageJ, U. S. National Institutes of Health, Bethesda, Maryland,

666 USA, http://rsb.info.nih.gov/ij/. 1997-2007.

667 42.   Abramoff, M.D., Magelhaes, P.J., Ram, S.J. "Image Processing with ImageJ".

668 Biophotonics International. 2004;11: 36—42.

669 **43.**   Kawaguchi Y, Hinoi T, Saito Y, Adachi T, Miguchi M, Niitsu H, et al. Mouse

670 model of proximal colon-specific tumorigenesis driven by microsatellite instability-

671 induced Cre-mediated inactivation of Apc and activation of Kras. J Gastroenterol.

43

672   2016;51: 447–457.

44.   Matsuda K, Tsuji H, Asahara T, Kado Y, Nomoto K. Sensitive quantitative

674   detection of commensal bacteria by rRNA-targeted reverse transcription-PCR. Appl

675   Environ Microbiol. 2007;73: 32–39.

45.   Matsuda K, Tsuji H, Asahara T, Matsumoto K, Takada T, Nomoto K.

677   Establishment of an analytical system for the human fecal microbiota, based on reverse

678   transcription-quantitative PCR targeting of multicopy rRNA molecules. Appl Environ

679   Microbiol. 2009;75: 1961–1969.

46.   Jansen GJ, Wildeboer-Veloo AC, Tonk RH, Franks AH, Welling GW.

681   Development and validation of an automated, microscopy-based method for enumeration

682   of groups of intestinal bacteria. J Microbiol Meth. 1999;37: 215–221.

47.   Grivennikov SI, Wang K, Mucida D, Stewart A, Schnabl B, Jauch D, et al.

684   Adenoma-linked barrier defects and microbial products drive IL-23/IL-17-mediated

685   tumour growth. Nature. 2012;491: 254–258.

48.   Fukuda S, Toh H, Hase K, Oshima K, Nakanishi Y, Yoshimura K, et al.

687   Bifidobacteria can protect from enteropathogenic infection through production of acetate.

688   Nature. 2011;469: 543–547.

49.   van Zanten GC, Knudsen A, Roytio H, Frorssten S, Lawther M, Blennow A, et al. The effect of selected synbiotics on microbial composition and short-chain fatty acid production in a model system of the human colon. PLoS One. 2012;7: e47212.

50.   Le Roy CI, Stsepetova J, Sepp E, Songisepp E, Claus SP, Mikelsaar M. New insights into the impact of *Lactobacillus* population on host-bacteria metabolic interplay. Oncotarget. 2015;6: 30545–30556.

51.   Marino F, Orecchia V, Regis G, Musteanu M, Tassone B, Jon C, et al. STAT3beta controls inflammatory responses and early tumor onset in skin and colon experimental cancer models. Am J Cancer Res. 2014;4: 484–494.

52.   Schneider MR, Hoeflich A, Fischer JR, Wolf E, Sordat B, Lahm H. Interleukin-6 stimulates clonogenic growth of primary and metastatic human colon carcinoma cells. Cancer Letts. 2000;151: 31–38.

53.   Carothers AM, Davids JS, Damas BC, Bertagnolli MM. Persistent cyclooxygenase-2 inhibition downregulates NF-κB, resulting in chronic intestinal inflammation in the min/+ mouse model of colon tumorigenesis. Cancer Res. 2010;70:

45

704   4433–4442.

705   **54.**   Thun MJ, Namboodiri MM, Heath CW. Aspirin use and reduced risk of fatal

706   colon cancer. N Engl J Med. 1991;325: 1593–1596.

707   **55.**   Dannenberg AJ, Altorki NK, Boyle JO et al. Cyclo-oxygenase 2: A

708   pharmacological target for the prevention of cancer. Lancet Oncol. 2001;2: 544–551.

709

Supporting information

711   **S1 Table. Disease activity score assessment (maximum score 12).**

712   **S2 Table. Histopathological scoring (maximum score 11).**

713   NC3Rs ARRIVE Guidelines Checklist.

714

46
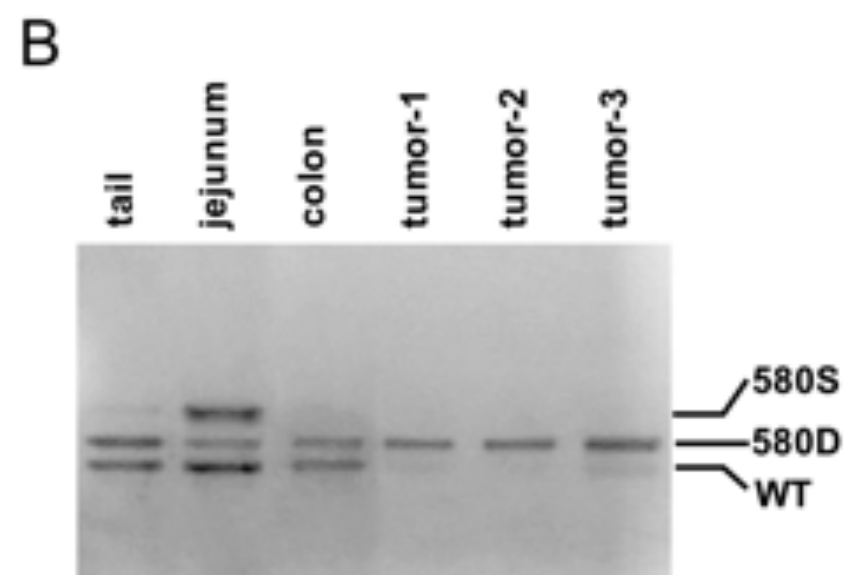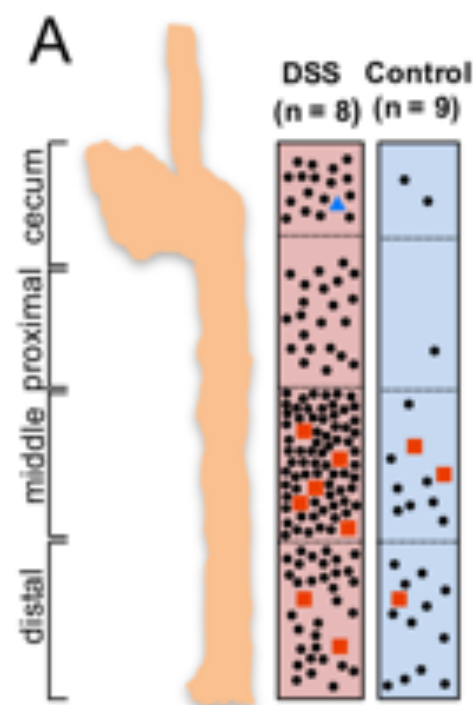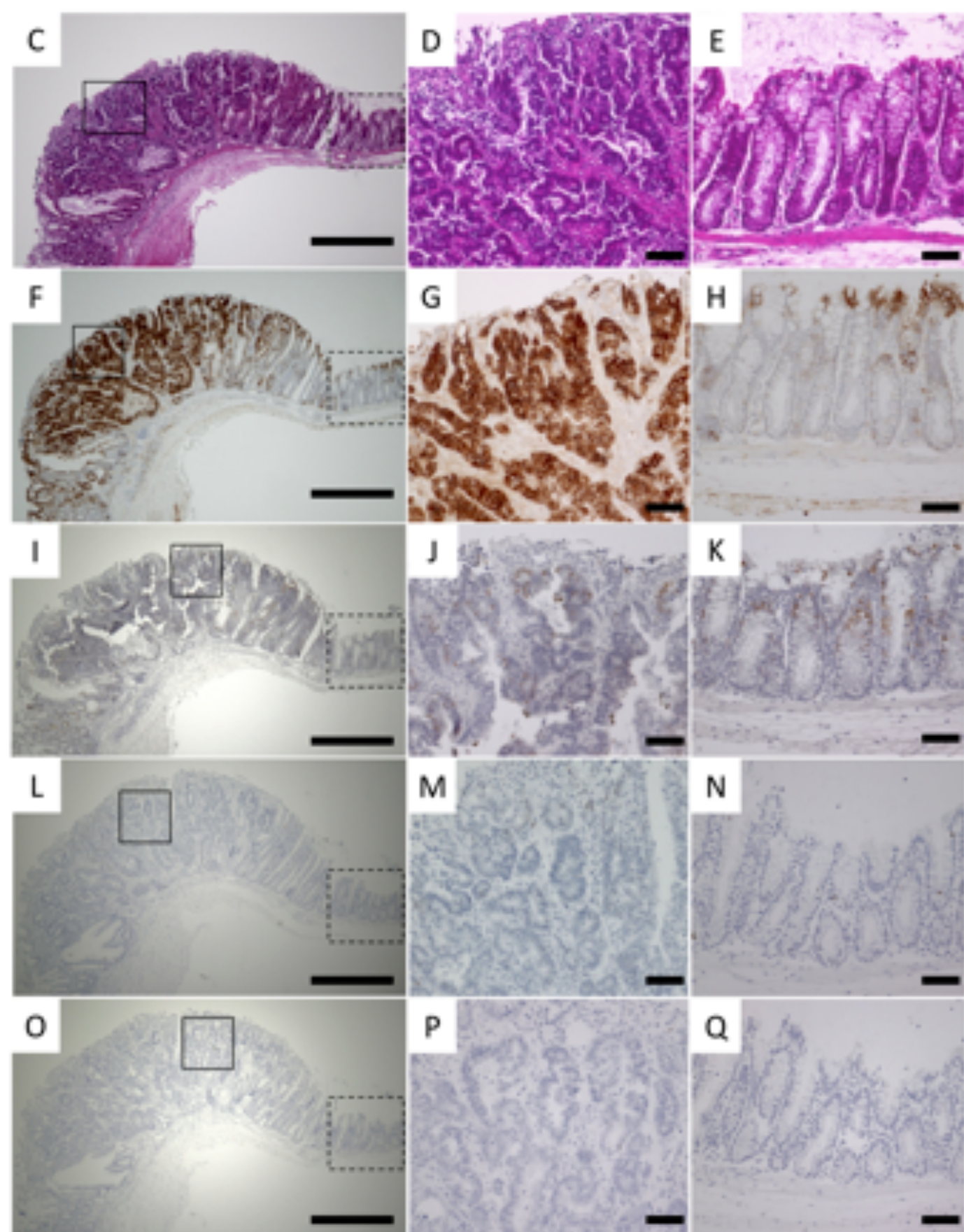
Fig. 1-a   Saito Y et al.

Fig.1-b   Saito Y et al.
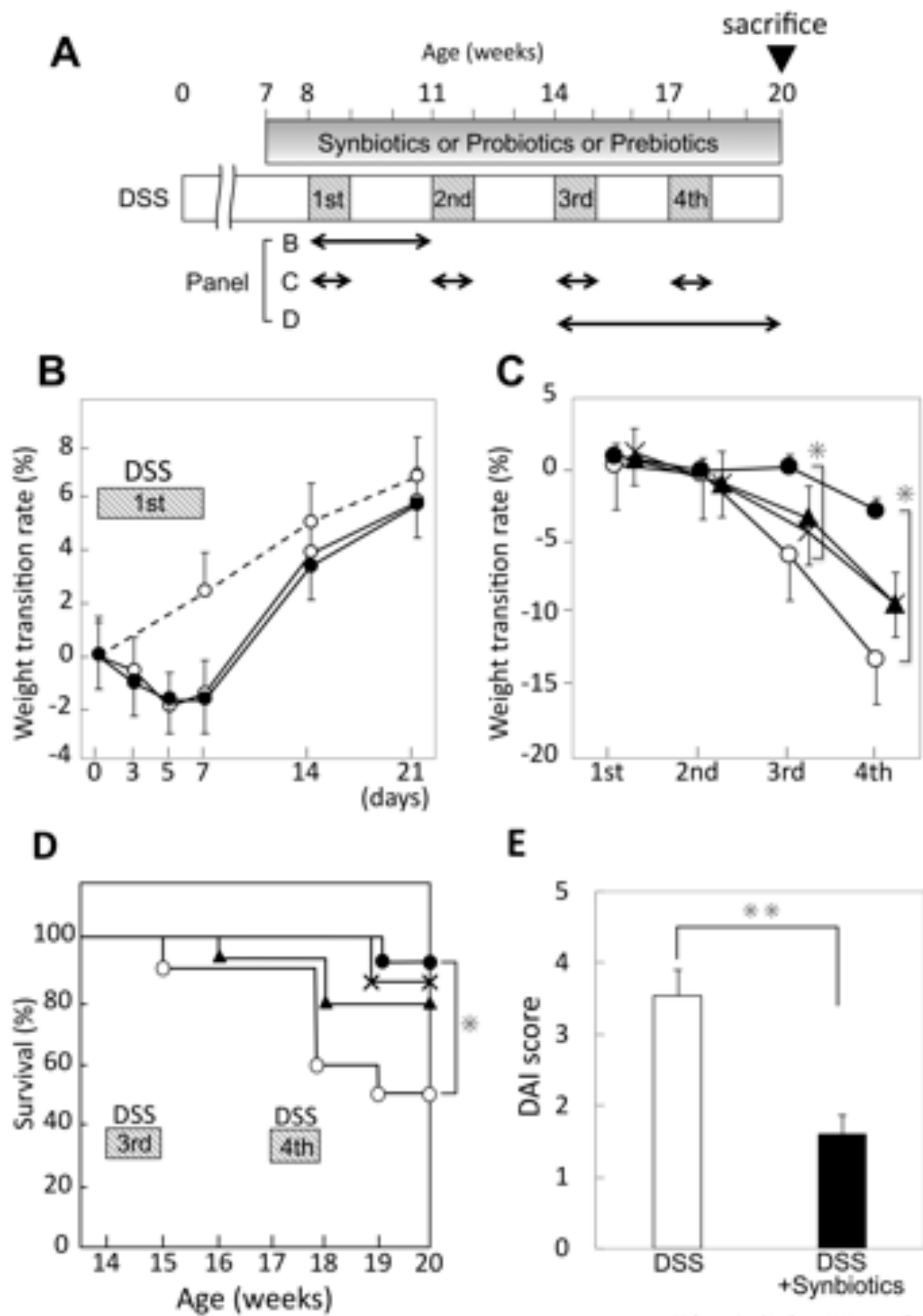
Fig. 2 Saito Y et al.

Fig. 3 Saito Y et al.

Control　　　**DSS**　　　**DSS + Synbiotics**
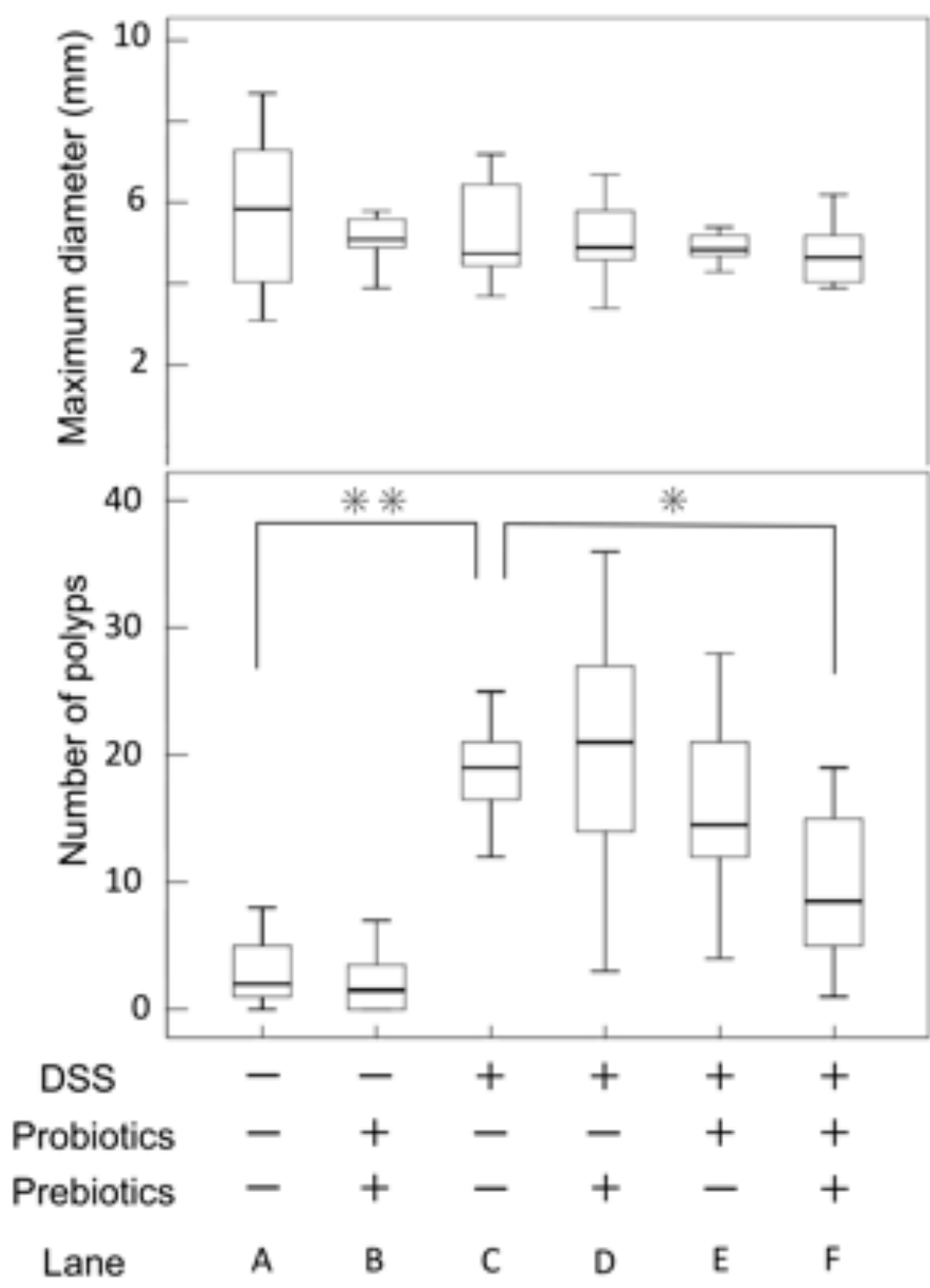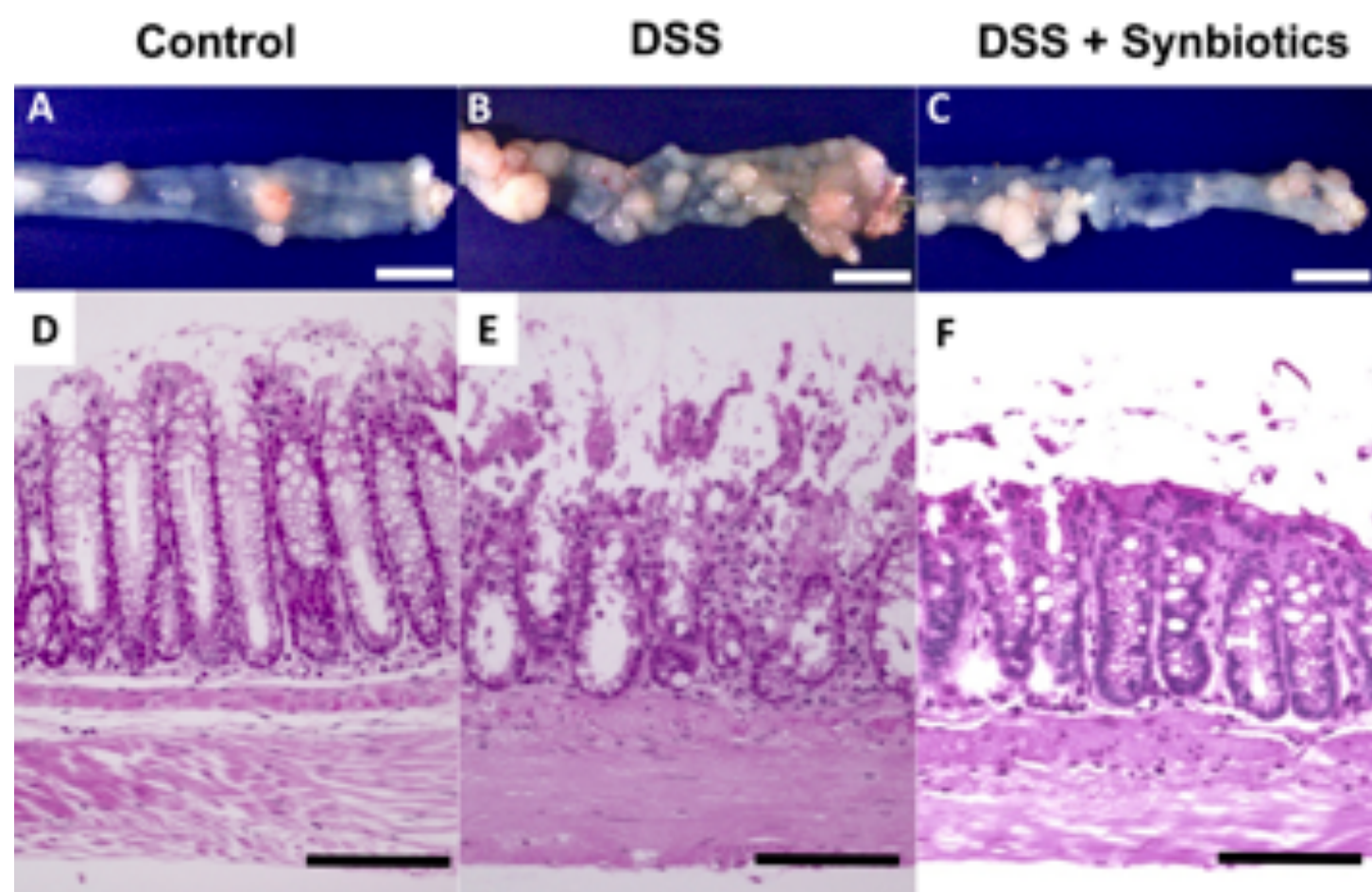
G　Histological Score
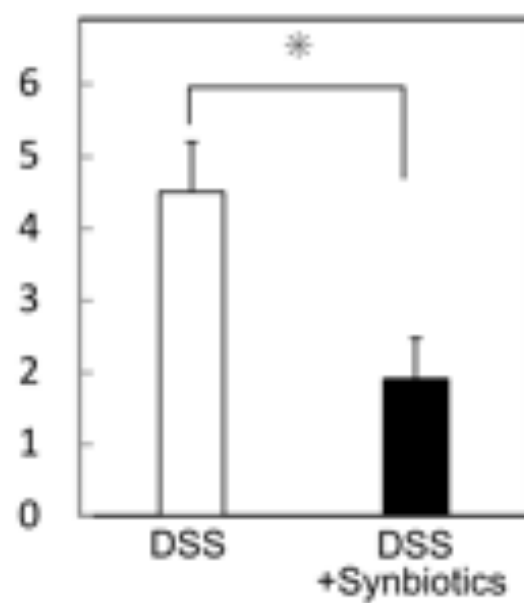
Fig. 4 Saito Y et al.
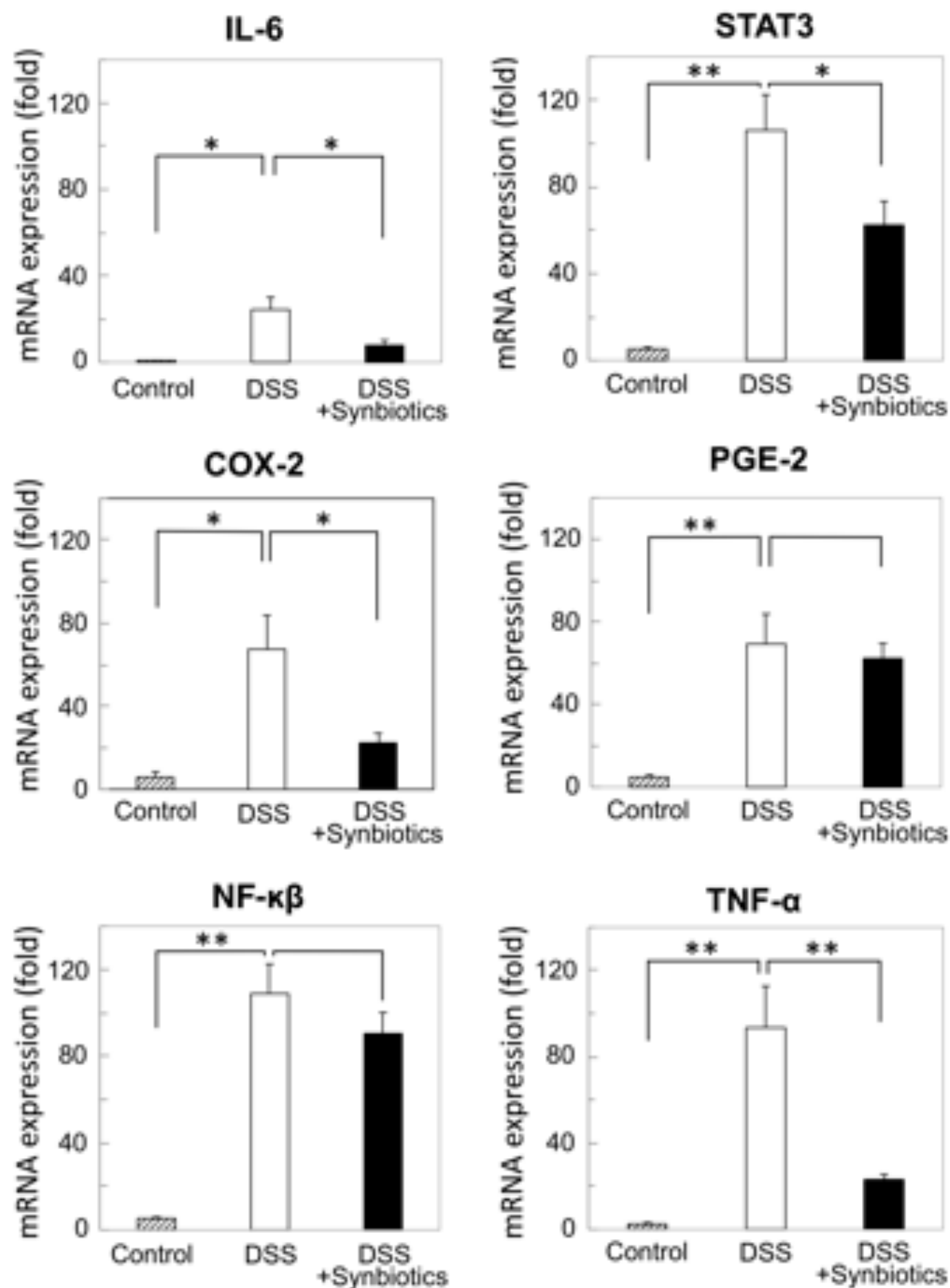
Fig. 5 Saito Y et al.

You are being carbon copied ("cc:'d") on an e-mail "To" "Takao Hinoi" thinoi@hiroshima-u.ac.jp
CC: "Yasufumi Saito" ngywc515@ybb.ne.jp, "Tomohiro Adachi" adachitomohiro@hotmail.com, "Masashi Miguchi" miguchima0815@gmail.com, "Hiroaki Niitsu" hiroaki_niitsu@yahoo.co.jp, "Masatoshi Kochi" msts.luv4@gmail.com, "Haruki Sada" z011028sangyo@yahoo.co.jp, "Yusuke Sotomaru" sotomaru@hiroshima-u.ac.jp, "Naoya Sakamoto" nasakamoto@hiroshima-u.ac.jp, "Kazuhiro Sentani" kzsentani@hiroshima-u.ac.jp, "Naohide Oue" naoue@hiroshima-u.ac.jp, "Wataru Yasui" wyasui@hiroshima-u.ac.jp, "Hirotaka Tashiro" htashiro@hiroshima-u.ac.jp, "Hideki Ohdan" hohdan@hiroshima-u.ac.jp

PONE-D-18-29054R1
Synbiotics suppress colitis-induced tumorigenesis in a colon-specific cancer mouse model

Dear Dr. Hinoi:

I am pleased to inform you that your manuscript has been deemed suitable for publication in PLOS ONE. Congratulations! Your manuscript is now with our production department.

If your institution or institutions have a press office, please notify them about your upcoming paper at this point, to enable them to help maximize its impact. If they will be preparing press materials for this manuscript, please inform our press team within the next 48 hours. Your manuscript will remain under strict press embargo until 2 pm Eastern Time on the date of publication. For more information please contact onepress@plos.org.

For any other questions or concerns, please email plosone@plos.org.

Thank you for submitting your work to PLOS ONE.

With kind regards,

PLOS ONE Editorial Office Staff
on behalf of

Professor Hossam MM Arafa
Academic Editor
PLOS ONE

_____